A thermal model for large mass TeO_2 bolometers with NTD Ge thermistors

Andrea Giuliani

Sezione di Milano dell'INFN, Via Celoria 16, I-20133 Milano, Italy

Abstract

We have developed a thermal model able to predict with reasonable accuracy the pulse structure of large mass TeO_2 bolometers operated with NTD Germanium thermistors. Some of the free parameters of the model (typically, thermal conductances of detector elements) were determined with *ad hoc* measurements. The model predictions are compared with real pulses and are used for the design of future detectors to be employed in the CUORICINO and CUORE projects.

1 Introduction

Purpose of this paper is to show that we have got a significant comprehension of our TeO_2 detector behaviour in terms of their basic thermal parameters; this achievement can be employed for the design and for the optimization of the CUORICINO and CUORE elements.

2 Description of the thermal model

The Thermal Model (TM) considered here assumes naively that the detector can be described as three thermal "nodes" with finite heat capacities (TeO_2 crystal absorber, Ge thermistor lattice, Ge thermistor electrons), connected among them and to the heat sink by means of thermal conductances. In order to simplify the evaluation of the thermal pulse, the node corresponding to the Ge thermistor lattice is supposed to have a negligible heat capacity with respect to the other two nodes. The network describing the detector is represented in figure 1. Input parameters for the model are the two relevant heat capacities and four thermal conductances (with their temperature behaviours), the parasitic power dissipated in the TeO_2 crystal by vibrations

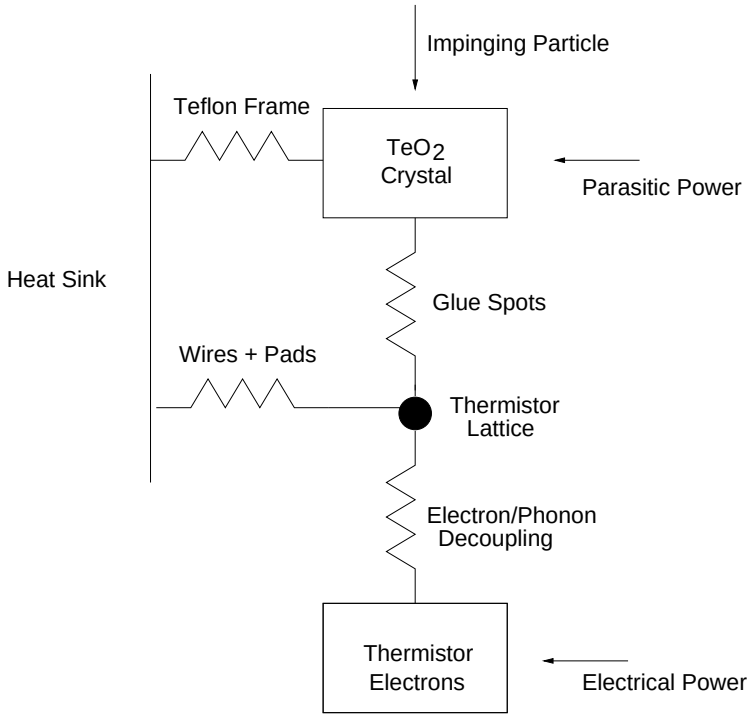

Fig. 1. Detector "network" with relevant thermal elements.

and the electrical power dissipated in the thermistor electrons for the signal read-out. For the pulse evolution, one assumes that a certain energy (typically, 1 MeV) is deposited in the TeO_2 crystal and istantaneously thermalized: this hypothesis is justified by the long (tens-hundreds of ms) intrinsic detector time constants.

2.1 The static behaviour

The static behaviour of the detector is determined by a program developed by Oliviero Cremonesi named CLOAD which operates as follows: the program requires as input data the heat sink temperature, the temperature behaviour of the thermal conductances appearing in figure 1, the parasitic power in the TeO_2 crystal and a set of electrical joule powers dissipated in the thermistor electrons for the redout. For each electrical power, the program solves completely the static problem and therefore outputs the following detector parameters (collectively indicated as *operation point*): temperatures of the three thermal nodes; resistance of the thermistor (the R-T curve of the themistor is known); current through the thermistor. A set of different operation points for the same detector, once fixed the heat sink temperature, is indicated as a *load curve*. A load curve can be expressed in terms of thermistor parameters, typically as a set of Voltage-Current or Power-Resistance points.

The determination of an operation point is not trivial, since the dissipated powers are so large to determine substantial temperature differences among the thermal nodes, of the same order of magnitude of the heat sink temperature. The determination of an operation point implies the simultaneous solution of three non linear coupled equations (detailed balance of the powers at each node); each power flowing between two nodes is an integral over the temperature difference between the two nodes of the thermal conductance connecting the nodes. For more detail about the numerical determination of the static solution, contact Oliviero Cremonesi.

2.2 The dynamical response

The principle at the base of the present model, which allowed to performe thousands of dynamical simulation in a reasonable CPU time, is that the pulse development is a small perturbation of a certain operation point determined by CLOAD. The perturbation is induced by an energy release in the TeO_2 crystal; "small" perturbation means that every time an integral of the following type appears:

$$\int_{T_0}^{T_s+\Delta T} G(T)\,\mathrm{d}T \tag{1}$$

where T_0 is the zero static power temperature, T_s is the temperature determined by the static powers and ΔT is the temperature change during pulse evolution, the integral in eq. 1 can be written in the following way:

$$\int_{T_0}^{T_s} G(T)\,\mathrm{d}T + \int_{T_s}^{T_s+\Delta T} G(T)\,\mathrm{d}T \simeq \int_{T_0}^{T_s} G(T)\,\mathrm{d}T + G(T_s)\cdot\Delta T \tag{2}$$

The approximation contained in eq. 2 allows to express the dynamical equations in terms of heat capacities and thermal conductances evaluated at the operation point temperatures; therefore, the dynamical equations are simply coupled linear equation with constant coefficients, having trivial solutions expressed by a sum of exponentials and analytically evaluable once the operation point is determined by CLOAD. Of course, it is assumed that the temperature behaviour of the heat capacities is known. Even the electrothermal feedback is taken into account introducing a proper effective thermal conductance. The analytical solution is very similar to the one obtained by the numerical solution of the differential equations. For more details about the analytical solution of the dynamical problem, contact Andrea Giuliani.

3 A criterium for the comparison of detector performances

It is not obvious to compare the performances of two different detectors. The trivial criterium consisting in comparing the respective pulse amplitudes for the same energy deposition requires some discussion. In general, thermistors with higher sensitivities and resitances give higher pulses, but this does not imply necessary better performances, since higher resistances are responsible also for higher sensitivity to spurious noise (microphony, cross talks, and slow heat pulses with triangular shape, familiarly nick-named "triangoloni" - large triangles - , which excite the very low frequency part of the noise spectrum, 1-5 Hz). Even the operation of a given detector at lower heat sink temperatures gives higher pulses, but at the price of a higher resistance and therefore of worse spurious noise.

Therefore, our recent experience has shown that the most significant way to define a merit figure for a detector is as follows. A heat sink temperature is fixed, typically between $\sim$6 mK and $\sim$13 mK. A load curve is measured at this heat sink temperature; by means of particle or heater pulses, the operation point on the load curve which corresponds to the highest signal is determined. For each heat sink temperature, one determines therefore a couple of points (Thermistor Resistance R, Signal Amplitude V, usually expressed in μV/MeV) corresponding to the maximum pulse amplitude for a given heat sink temperature. This operation is repeated for several heat sink temperatures. If all the R-V points are then plotted with R on the X-axis and V on the Y-axis, one obtains a characteristic curve for that detector, which is with a good approximation a straight line in a log-log plot. This curve is familiarly referred to as "Pirro Curve". Our experience shows that a detector has a very similar behaviour in terms of S/N ratio along a Pirro Curve: it does not make a big difference to work at a heat sink temperature of, say, 8 mK or 12 mK: what you lose in signal, you gain in spurious noise, and vice versa. Usually, it is better to avoid the exetremities of the Pirro Curve, which lead respectively to too high spurious noise or to too small signals.

It is now obvious that a meaningful way to compare two different detectors is *to compare their Pirro Curves*: if in an R-V space the Pirro Curve of detector A lies systematically above the Pirro Curve of detector B, detector A is "better" than detector B; in other terms, the best detector is the one which provides highest signals for the *same* thermistor resistance value. An example of two real detectors compared through their Pirro Curves is shown in fig. 2. In this case, the best detector has a larger thermistor volume.

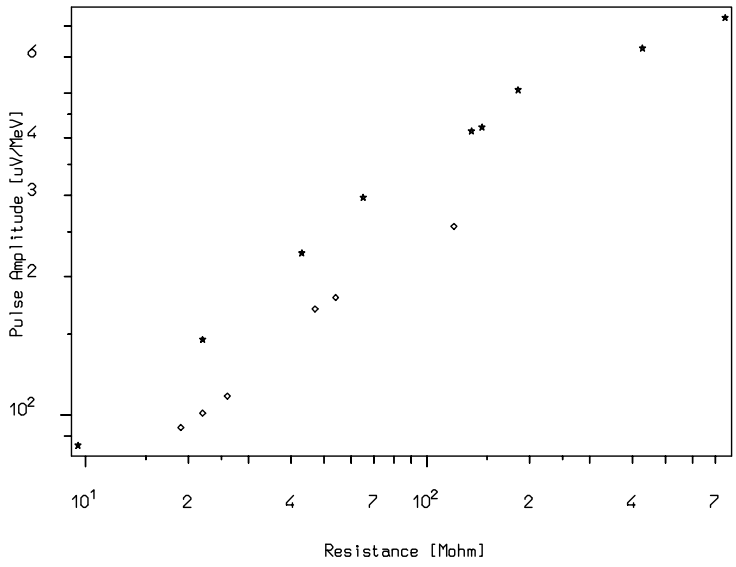

Fig. 2. Two Pirro Curves for two different detectors.

4 Interpretation of the real detector behaviour by means of the model

The main aim of the TM is therefore to predict the Pirro Curve of a detector, given its constructive parameters. It is then possible to optimize the detector construction.

4.1 Choice and evaluation of the basic model parameters

The quantities required to define completely a detector in the present TM are the following [1]:

- thermistor characteristic curve, expressed in terms of the Variable Range Hopping parameters R_0, T_0 and γ;
- background power acting on the crystal, presumably for vibrational heating (we assume presently 6.5 pW for this parameter since it describes satisfactorily the detector behaviour, but it should be determined better in the future by means of specific measurements);
- glue spot thermal conductance, expressed by the relationship (Milano Group measurement):

$$G_{\text{glue spot}}[\text{W/K}] = 2.6 \times 10^{-4} T[\text{K}]^3; \tag{3}$$

the glue spots are used to connect the thermistor to the crystal [2];

- thermal conductance of the thermistor lattice to the heat sink, probably offered by the interface between thermistor and gold pads (and so proportional to pad area) and expressed by (Milano Group measurement):

$$G_{\text{gold pad}}[\text{W}/(\text{K}\cdot\text{mm}^2)] = 1.6\times10^{-5}T[\text{K}]^{2.4}; \tag{4}$$

- thermal conductance of the crystal to the heat sink, offered by the teflon frame [2] and expressed by (Milano Group measurement):

$$G_{\text{teflon frame}}[\text{W/K}] = 4\times10^{-5}T[\text{K}]^{2}; \tag{5}$$

- electron-phonon conductance inside the thermistor itself, taken as:

$$G_{\text{electron}-\text{phonon}}[\text{W}/(\text{K}\cdot\text{mm}^3)] = 7.8\times10^{-2}T[\text{K}]^{4.37}; \tag{6}$$

  this parameter was measured by the Milano Group in a special set up [1] and slightly corrected to account for the real shape of the load curves measured in the detectors of the presently operating array;
- TeO_2 crystal specific heat (it is assumed the Debye Law with $\Theta_D = 270$ K);
- thermistor electron specific heat, given by

$$C_{\text{thermistor electrons}}[\text{J}/(\text{K}\cdot\text{mm}^3)] = 1.1\times10^{-9}T[\text{K}]; \tag{7}$$

  this relationship was not measured separately, but chosen to account for the observed rise times: a direct measurement should be included in future plans;

We admit that all these parameters would require further investigations and other specific measurements in order to constrain more effectively the TM and refine its predictive properties. A measurement program should be studied in the CUORE collaboration for this purpose.

4.2 Test of the model with real detectors

The test of the model was performed as follows. A typical detector of the presently operating array was simulated, introducing the present thermistor geometry and characteristic curve, the present glue spot number and the present crystal volume. A Pirro Curve was then constructed using the TM for this detector. This *simulated* Pirro Curve was then compared to the *real* Pirro Curves collected for the 20 detector array. A significant spread is present among the experimental points (which refer to all the 20 detectors together) for two reasons: intrinsic detector irreproducibility and presence of points not corresponding exactly to the maximum signal. Nevertheless, one can appreciate that the simulated Pirro Curve lies inside the experimental points and has the correct slope (see fig. 3): in other terms, the simulated detector is not

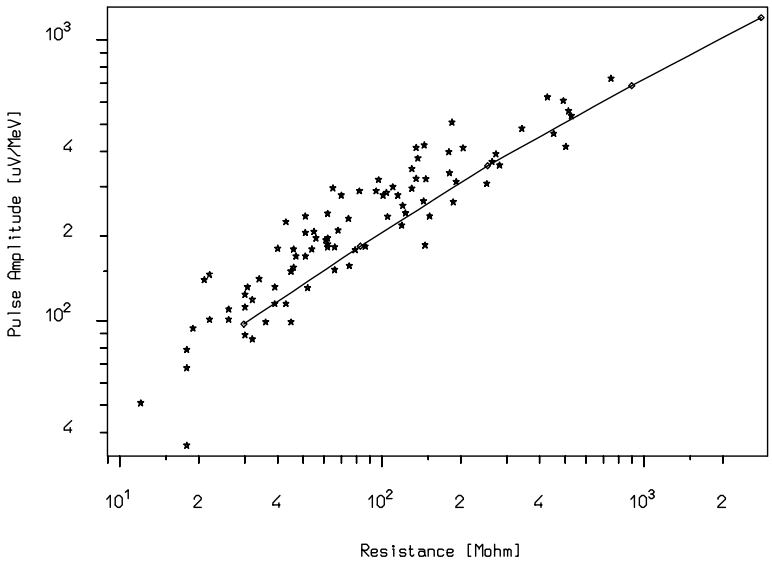

Fig. 3. A simulated Pirro Curve (solid line) compared with the R-V points of the 20 detector array.

distinguishable by a typical array detector. Of course, not only the pulse amplitude, but also the time constants must be correctly predicted by the TM. At a typical operating resistance of about 100 MΩ, the predicted rise time (10 % - 90 %) and decay time (90 % - 10 %), which are respectively 40 ms and 430 ms, lies inside the distribution of these parameters for the 20 detector array [3]. In fig. 4, the simulated pulse is compared with real pulses collected with four detectors randomly chosen among the twenty elements: it is evident that, even from the point of view of pulse shape, the simulated detector can be confused with a typical array detector. It is interesting also to see how the simulated pulses change by varying the base temperatures (fig. 5). We conclude therefore that the TM is able to explain the typical detector of the present array . A further test of the model was performed on a detector different from the typical ones for two aspects: the thermistor geometry was changed (section of 3×1 mm^2 instead of 1.5×0.4 mm^2) and 12 glue spots instead of 6 were used. The model overestimates slightly the signal amplitude (fig.6), but in any case it provides a satisfactory indication on how the detector response changes in this new situation.

5 Future detector design by means of the model

Once the TM was tested, a systematic study was carried out to see how the conctructive parameters must be changed in order to improve the detector performances. This study was performed as follows. Given a set of constructive

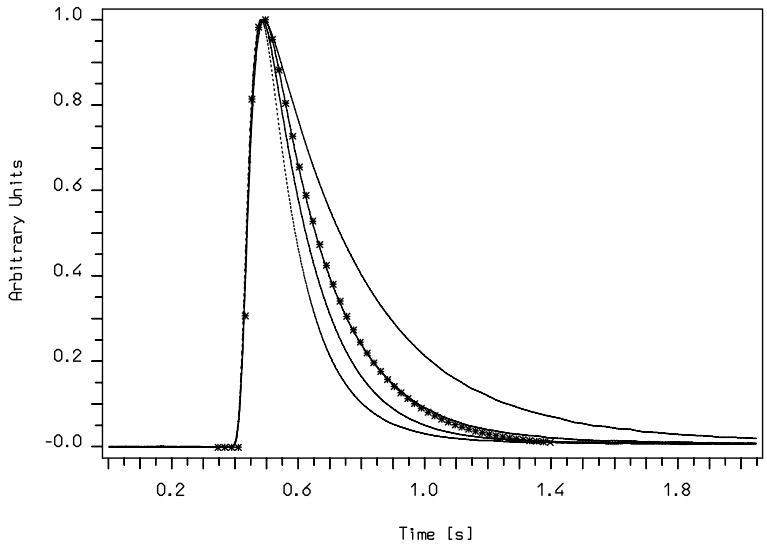

Fig. 4. A simulated pulse (points) compared with real pulses (lines) from four array elements (the pulses are normalized in amplitude).

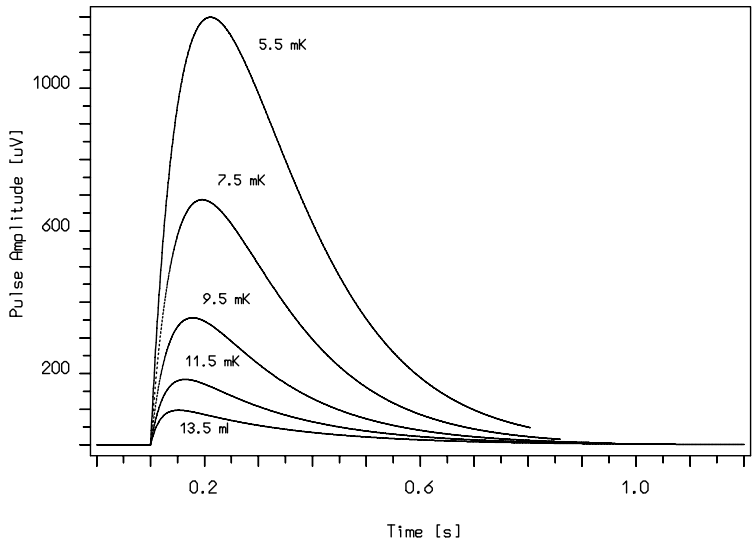

Fig. 5. Simulated pulses at different heat sink temperatures for the present array detectors.

parameters, included in a proper input file, a procedure constructs (by means of CLOAD) 5 load curves at the base temperatures 5.5 mK, 7.5 mK, 9.5 mK, 11.5 mK and 13.5 mK. For each load curve, the dynamical simulation allows to establish the operation point at which the signal amplitude is maximum. An n-tuple of data for each maximum is then produced, including the following

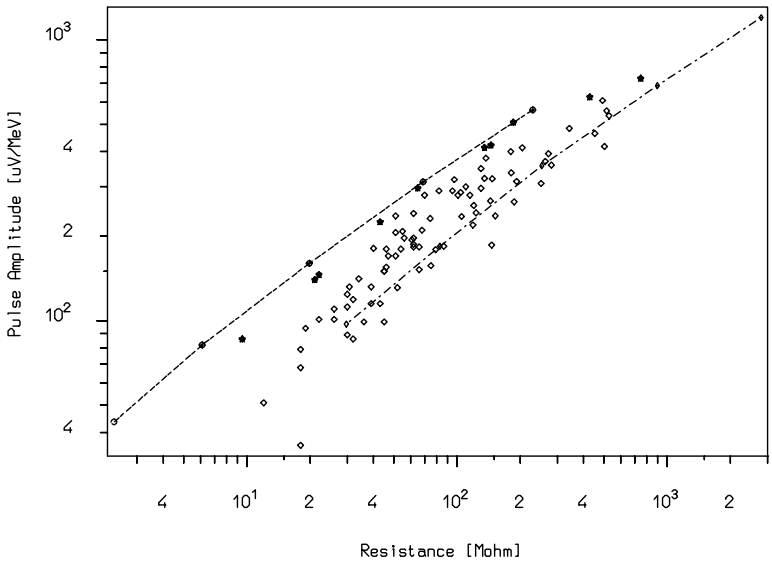

Fig. 6. Pirro Curves for array detectors (diamonds) and large thermistor detector (stars): the solid lines are the corresponding simulations.

parameters (and others less relevant):

1) Operation Resistance;
2) Pulse Amplitude for 1 MeV deposited energy;
3) Voltage across the thermistor;
4) Operation Thermistor Temperature;
5) Rise Time (10 % - 90 %);
6) Fall Time (90 % - 10 %);

The first two parameters, when plotted for each base temperature, sample the Pirro Curve; the other parameters complete the informations about the detector performances. In order to compare two detectors with two different sets of constructive parameters, it is important to establish the values of parameters from 2 to 6 at a *fixed* resistance value (typically around 100 MΩ). For this purpose, linear fits in a log-log space of the parameters 2 through 6 as a function of the operation resistance (taken as the basic independent variable) are performed. The heat sink temperature is also fit as a function of the optimum operation resistance. Therefore, given a certain value for the operation resistance, it is possible to estimate the heat sink temperature for which the signal is maximum at that value; the corresponding values for the other parameters can also be determined. Now, if we want to compare detectors which differ for instance by the number of glue spots, this procedure can be carried out for a set of different glue spot numbers; then, at a fixed value of the operation resistance, the pulse amplitude can be studied as a function of the glue spot number, and the other parameters can also be determined.

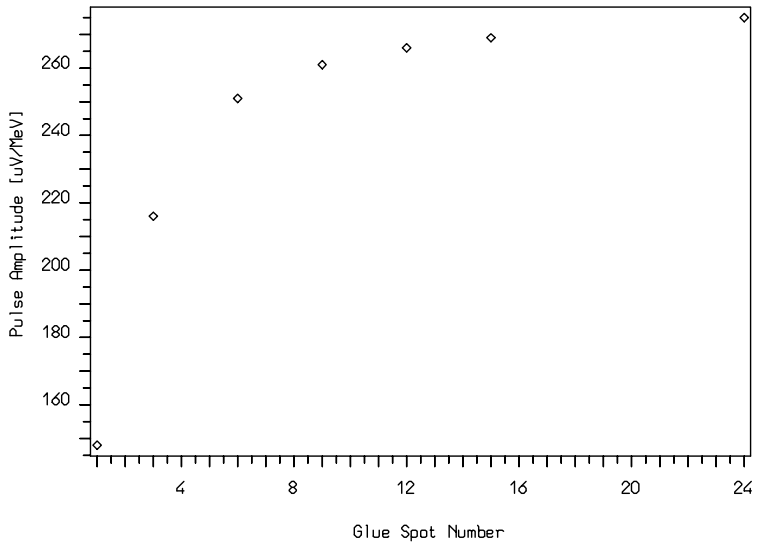

Fig. 7. Pulse Amplitude as a function of the Glue Spot Number, for a fixed resistance value (150 MΩ).

5.1 Requirements on constructive detector parameters

Two constructive parameters were studied according to the procedure described above: the glue spot numbers and the thermistor conductance to the heat sink (gold pad area). The philosophy is to start from a typical present array detector and vary the parameter under study fixing the others. In this first phase, the delicate correlations among the various parameters are therefore not examined.

Glue spot numbers. The results are reported in fig. 7 and 8. Looking at fig. 7, it is clear that there is an initial large improvement by increasing the glue spot number, but no substantial signal increase is expected starting from the present value of 6. This has a simple explanation: increasing the glue spot number, the phonon-electron decoupling becomes more and more important with respect to the decoupling offered by the glue. The curve explains why we got a significant increase in signal amplitude passing from the first generation 3 spot detectors to the present 6 spot detectors. The corresponding decreasing of the rise time can be appreciated in fig. 8.

Gold pad area. The results are reported in fig. 9. As expected, the decreasing of the thermistor conductance to the heat sink improves detector performances. The ideal would be to make this conductance negligible with respect to the other ones, in particular to the phonon-electron conductance.

5.2 Requirements on NTD thermistor properties

Two effects have been for the moment studied: variation of thermistor volume and variation of thermistor sensitivity through the VRH parameter T_0.

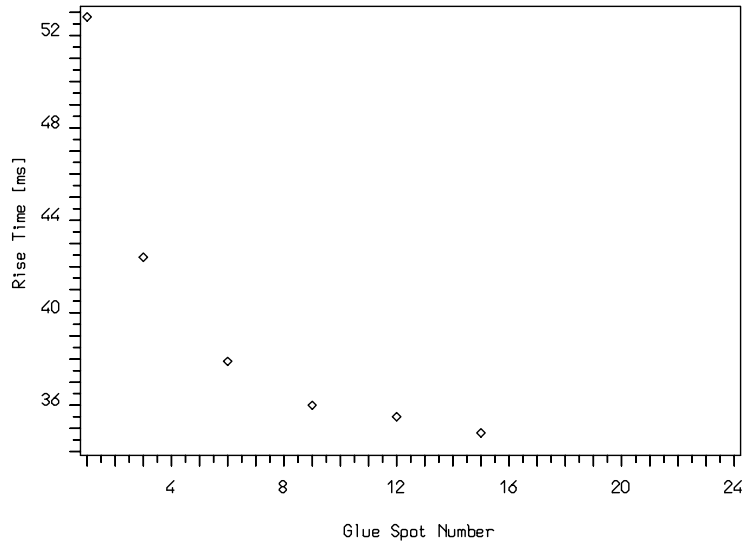

Fig. 8. Rise Time as a function of the Glue Spot Number, for a fixed resistance value (150 MΩ).

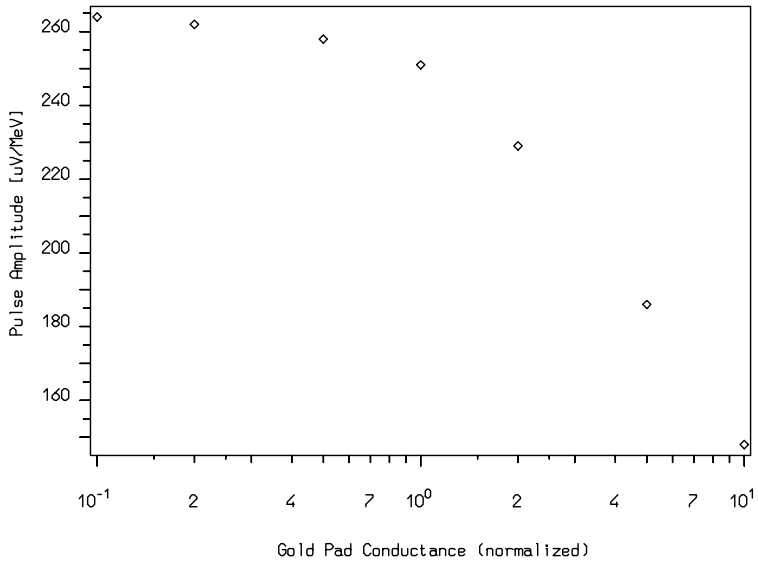

Fig. 9. Pulse Amplitude as a function of the thermistor conductance to the heat sink (normalized with respect to the present value), for a fixed resistance (150 MΩ).

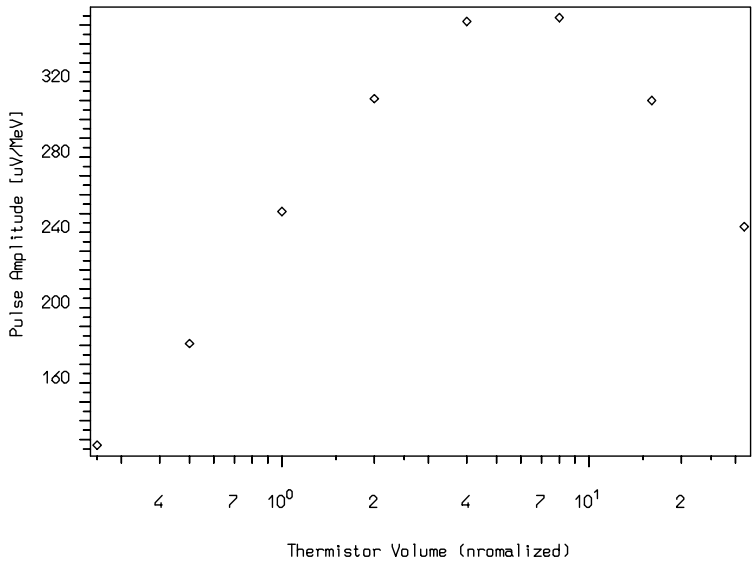

Fig. 10. Pulse Amplitude as a function of Thermistor Volume (normalized with respect to the present value), for a fixed resistance (150 MΩ).

Thermistor Volume. It has been varied keeping constant the distance between the contact (3 mm). Therefore, its variation has implied not only the variation of the parameters directly connected to the volume (thermistor heat capacities and phonon-electron decoupling) but also the variation associated to the cross section of the thermistor: R_0 and the gold pad area. The results are exposed in fig. 10 and 11, showing the fixed resistance pulse amplitudes and rise times respectively. An optimum for the volume exists: it is about an order of magnitude higher than the present volume. Even better results could be achieved if one could increase the volume without increasing simultaneously the thermistor conductance to the heat bath. The existance of an optimum value is due to the fact that small volumes imply high electron-phonon decoupling, while large volumes imply both large thermistor heat capacity and large thermistor coupling to the bath. The rise time remains reasonable even for volumes 10 times higher than the present one.

Thermistor Sensitivity. We have assumed a thermistor with $T_0 = 2.5$ K instead of the present $T_0 = 3.3$ K. Unfortunately, at our knowledge, unlike silicon implanted thermistors, for NTD thermistors there is no systematic reliable study of the phonon-electron conductance as a function of T_0. We have therefore rather arbitrarily (and optimistically!) assumed that the phonon-electron conductance be twice in $T_0 = 2.5$ K thermistors with respect to the present $T_0 = 3.3$ K thermistors. The same R_0 is assumed for the same geometry. The CUORE collaboration should consider to measure systematically the phonon-electron decoupling as a function of T_0 in NTD Ge thermistors. The results, exposed in fig. 12 is encouraging: the pulse amplitude as a function of the thermistor volume is shown (acting as usual on

thermistor cross section and fixing at 3 mm the contact distance) and compared with the analogous relationship for $T_0 = 3.3$ K thermistors. About a factor two in signal amplitude could be gained. The improvement is so substantial that an analysis of lower T_0 thermistors is mandatory.

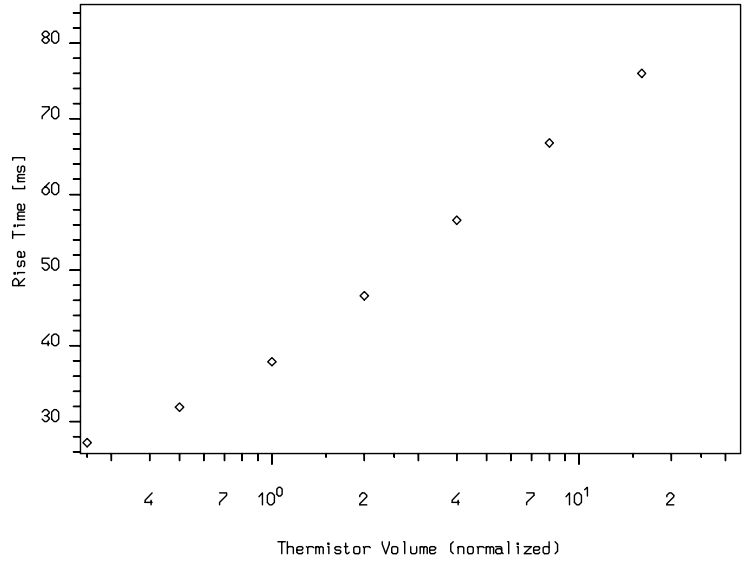

Fig. 11. Rise Time as a function of the Thermistor Volume (normalized with respect to the present value), for a fixed resistance (150 MΩ).

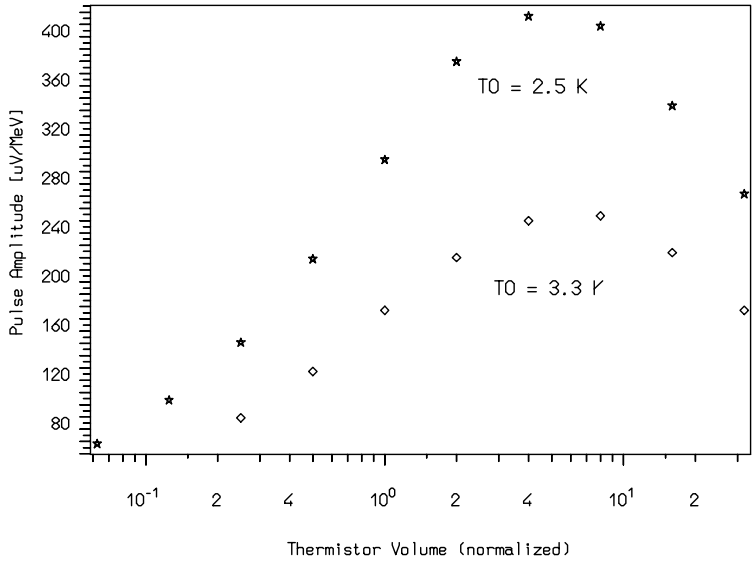

Fig. 12. Pulse Amplitude as a function of the Thermistor Volume (normalized with respect to the present value) for $T_0 = 3.3$ K and $T_0 = 2.5$ K thermistors at a fixed resistance (80 MΩ).

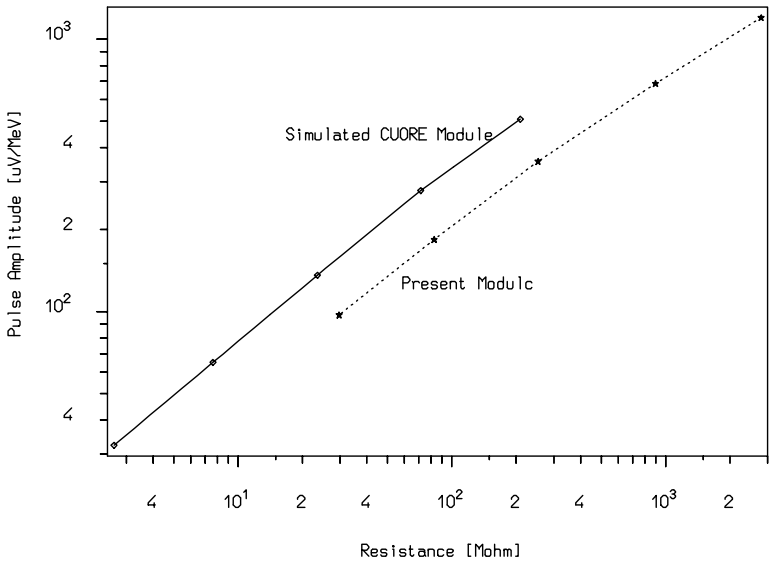

Fig. 13. Performance of a CUORE element compared with the present detector behaviour.

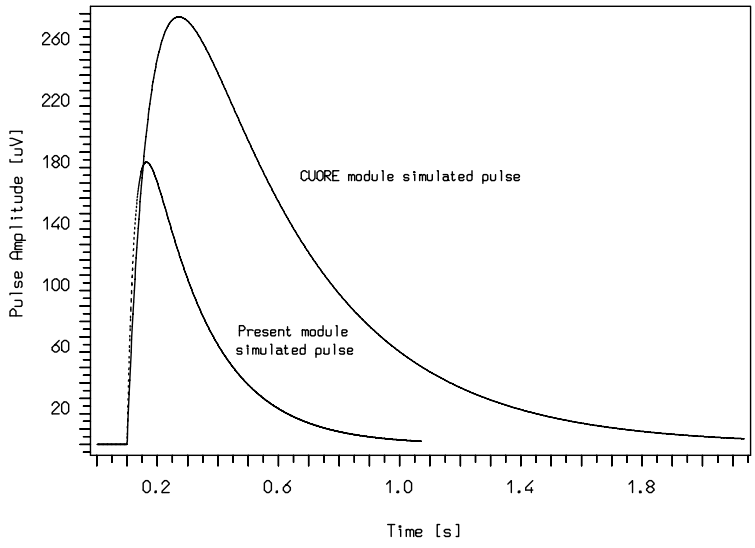

Fig. 14. CUORE module simulated pulse compared with present pulse (1 MeV energy deposition, ~80 MΩ thermistor resistance).

6 Conclusions

The results exposed above suggest to employ for CUORICINO and CUORE projects detectors of this type:

TeO_2 crystal. The sensitive mass will be 750 g instead of the present 340 g;

Crystal holder. We propose a teflon based method similar to the present one [2], introducing a similar thermal conductance; for the moment, no systematic study on this parameter was performed;

Thermistor wires. Aluminum wires should be used instead of the present gold wires, in order to minimize the thermistor conductance to the bath; in this case the thermistor gold pad heat capacity would add to the thermistor lattice heat capacity, that should however remain negligible with respect to the electron heat capacity due to pad thinness. Unfortunately, the use of aluminum wires would imply a major change in the detector mounting procedure;

Thermistor volume. We propose thermistors with $T_0 = 3.3$ K like the present ones (series # 31) but with size $1.5 \times 4 \times 3$ mm^3 (contact distance 3 mm) giving a volume 10 times larger than the present one;

Glue spot number. The surface 3×4 mm^2 of the thermistor should easily accomodate 15 glue spots;

Thermistor sensitivity. In parallel with the above described thermistor properties, lower sensititivity thermistors should be taken into account, in order to estimate the real influence of the improved phonon-electron coupling; we propose thermistor of the same volume and geometry, but with $T_0 = 2.5$ K.

In fig. 13 we compare a CUORE element realized on the basis of these considerations with the present array element. Improvement of a factor 1.5 of signal amplitude for the same resistance value looks possible, in spite of a mass more than twice larger. Better results might be achieved with lower T_0 thermistors. The pulses of the present module and of the planned CUORE module are compared in fig. 14: the base temperature is 7.5 mK in the CUORE case and 11.5 mK in the present case, so that in both cases the operation resistance is about 80 MΩ. The longer time constants in the CUORE case are evident, due to both crystal and thermistor larger size.

References

[1] Czechoslovak J. Phys. **46** (1996) 2893, Suppl. S5

[2] look at the WEB site *http://hpbbgs.lngs.infn.it/hallc/array.html*

[3] See presentation of CUORE at WEIN 98 (Santa Fe), C. Brofferio